Accuracy Improvement of a 5-axis Hybrid Machine Tool

Jun-Woo Kim*, Hye-Yoon Kim, and Han-Sung Kim

School of Mechanical Engineering and Automation,
Kyungnam University,
449 Wolyoung Dong, Masan, Kyungnam, 631-701, Korea (hkim@kyungnam.ac.kr)

Abstract

In this paper, a novel 5-axis hybrid-kinematic machine tool is introduced and the research results on accuracy improvement of the prototype machine tool are presented. The 5-axis hybrid machine tool is made up of a 3-DOF parallel manipulator and a 2-DOF serial one connected in series. The machine tool maintains high ratio of stiffness to mass due to the parallel structure and high orientation capability due to the serial-type wrist. In order to acquire high accuracy, the methodology of measuring the output shafts by additional sensors instead of using encoder outputs at the motor shafts is proposed. In the kinematic view point, the hybrid manipulator reduces to a serial one, if the passive joints in the *U-P* serial chain at the center of the parallel manipulator are directly measured by additional sensors. Using the method of successive screw displacements, the kinematic error model is derived. Since a ball-bar is less expensive than a full position measurement device and sufficiently accurate for calibration, the kinematic calibration method of using a ball-bar is presented. The effectiveness of the calibration method has been verified through the simulations. Finally, the calibration experiment shows that the position accuracy of the prototype machine tool has been improved from 153 to 86 [μm].

1 Introduction

A Conventional 5-axis machine tool provides high accuracy and large workspace. However, due to the serial-kinematic structure, it generally requires very massive structure to maintain high stiffness. In order to increase the ratio of stiffness to mass, the 3-DOF parallel-kinematic manipulator is employed as an arm and for high orientational capability, the 2-DOF serial-kinematic manipulator is used as a wrist. Hence, the proposed machine tool has a 5-DOF hybrid- kinematic structure as shown in Fig. 1. This machine tool will be applied for both machining and assembling tasks of automobiles' cylinder blocks. Specifically, the parallel manipulator has three *U-P-S* legs at the side and one *U-P* leg at the center, where the prismatic joints in the *U-P-S* chains are controlled by linear actuators and the prismatic joint in the *U-P* chain is passive.

In design and control of a machine tool, to obtain high accuracy is one of the most important tasks to be accomplished. In order to guarantee high accuracy, the methodology of measuring the output shafts by additional sensors instead of using encoder outputs at the motor shafts is proposed. For the parallel manipulator, we additionally install two angular encoders and one linear encoder at the *U-P* chain and two angular encoders at the output shafts of the serial manipulator as shown in Fig. 1. Therefore, we can calculate the position and orientation of the tool tip by the outputs of the five sensors connected in series. Hence, we can consider the hybrid manipulator as a serial manipulator, i.e., the *U-P-R-R* chain. In modeling kinematic errors, we used the method of successive screw displacements [1] instead of the Denavit-Hartenberg notations because the former is more general and straightforward [2].

Since a ball-bar is less expensive than a full position measurement device and sufficiently accurate for calibration, the kinematic calibration on the proposed machine tool will be performed by using a ball-bar. For a length measurement, i.e., using a ball-bar, the kinematic calibration is reduced to a nonlinear least square method of minimizing the calculated and measured lengths of a ball-bar. The effectiveness of the kinematic calibration method with a ball-bar is verified through the simulations. Through calibration experiment, the accuracy has been improved from 153 to 86 [μm].

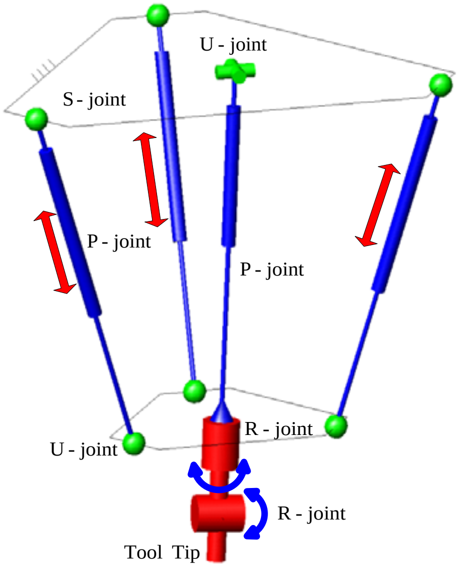

Fig. 1 Structure of the hybrid-kinematic machine tool.

2 Position Analysis

The forward kinematics of the machine tool can be obtained by considering the central leg, i.e., *U-P-R-R* serial chain in the middle if the *U-P* passive joints are measured. At a reference position, the kinematic parameters may be listed in Table 1, where $\boldsymbol{s}_i$ and $\boldsymbol{s}_{0i}$ denote the direction and location of the i^{th} joint axis with respect to the fixed coordinate system A(x, y, z) when the machine tool is at the reference position.

Substituting the coordinates of the joint axes into the equation of the general spatial displacement, known as *Rodrigues's formula*, the screw transformation matrices:

$$A_1 = \begin{bmatrix} 1 & 0 & 0 & 0 \\ 0 & c\theta_1 & -s\theta_1 & 0 \\ 0 & s\theta_1 & c\theta_1 & 0 \\ 0 & 0 & 0 & 1 \end{bmatrix},\ A_2 = \begin{bmatrix} c\theta_2 & 0 & s\theta_2 & 0 \\ 0 & 1 & 0 & 0 \\ -s\theta_2 & 0 & c\theta_2 & 0 \\ 0 & 0 & 0 & 1 \end{bmatrix},$$

$$A_3 = \begin{bmatrix} 1 & 0 & 0 & 0 \\ 0 & 1 & 0 & 0 \\ 0 & 0 & 1 & t_3 \\ 0 & 0 & 0 & 1 \end{bmatrix},\ A_4 = \begin{bmatrix} c\theta_4 & -s\theta_4 & 0 & 0 \\ s\theta_4 & c\theta_4 & 0 & 0 \\ 0 & 0 & 1 & 0 \\ 0 & 0 & 0 & 1 \end{bmatrix},$$

$$A_5 = \begin{bmatrix} c\theta_5 & 0 & s\theta_5 & -(L_0+L_1)s\theta_5 \\ 0 & 1 & 0 & 0 \\ -s\theta_5 & 0 & c\theta_5 & (L_0+L_1)(1-c\theta_5) \\ 0 & 0 & 0 & 1 \end{bmatrix}, \tag{1}$$

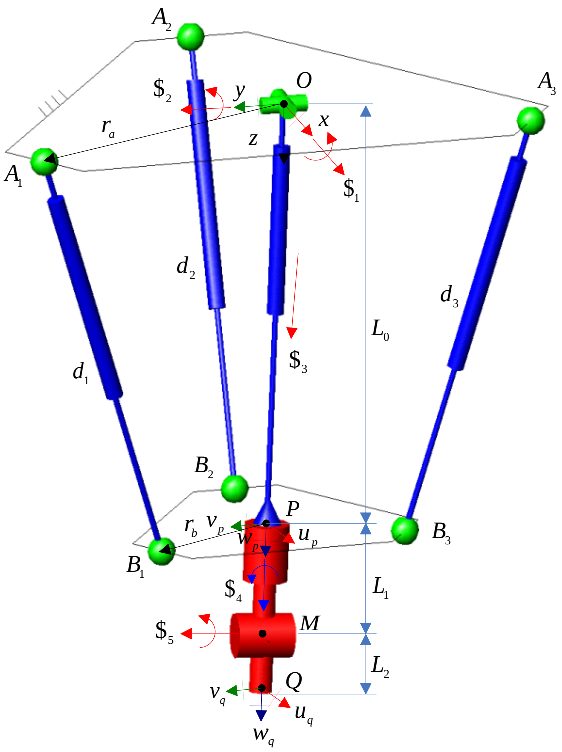

Fig. 2 Kinematic parameters of the machine tool.

Table 1 Screw axis locations and reference position.

Joint	$\boldsymbol{s}_i$	$\boldsymbol{s}_{0i}$
1	(1,0,0)	(0,0,0)
2	(0,1,0)	(0,0,0)
3	(0,0,1)	(0,0,0)
4	(0,0,1)	(0,0,0)
5	(0,1,0)	$(0,0,L_0+L_1)$

where $c\theta_i = \cos\theta_i$, $s\theta_i = \sin\theta_i$ and t_3 denotes the linear displacement of the prismatic joint in the middle of the machine tool.

The target position of the tool tip Q can be given by

$$\begin{bmatrix} R_q & \boldsymbol{q} \\ 0_{1\times3} & 1 \end{bmatrix} = A_1(\theta_1)A_2(\theta_2)A_3(t_3)A_4(\theta_4)A_5(\theta_5)\begin{bmatrix} I_{3\times3} & \boldsymbol{q}_0 \\ 0_{1\times3} & 1 \end{bmatrix} \tag{2}$$

where $\boldsymbol{q}_0 = [0,0,L_0+L_1+L_2]^T$ denotes the too tip Q when the machine tool is at the reference position. At the reference position, the orientation of the moving frame coincides with that of the fixed frame.

For the inverse kinematics of the *U-P-R-R* serial chain, only 5 of the 12 parameters associated with the end-effector position vector and rotation matrix can be specified at will. This is because the manipulator has only 5 degrees of freedom. In this work, the position vector ($\boldsymbol{q}$) and the approach vector ($\boldsymbol{w}_q$) are specified and the other two unit vectors, $\boldsymbol{u}_q$ and $\boldsymbol{v}_q$, are to be determined after the joint angles are found. The point M can be obtained by

$$\boldsymbol{m} = \boldsymbol{q} - L_2\boldsymbol{w}_q \tag{3}$$

We observe that the position of the point M depends only on the first three joint variables, θ_1, θ_2, and t_3. From the geometry, the direction vector and the travel distance of the prismatic joint is determined by

$$\boldsymbol{s}_3 = \boldsymbol{m}/\|\boldsymbol{m}\| \text{ and } t_3 = \|\boldsymbol{m}\| - (L_0+L_1) \tag{4}$$

Furthermore, the other two angles can be easily obtained in the following.

$$\boldsymbol{s}_3 = R_1R_2R_3\boldsymbol{w}_{q0} \text{ where } \boldsymbol{w}_{q0} = [0,0,1]^T \tag{5}$$

This equation reduces to

$$\begin{bmatrix} s_{3x} \\ s_{3y} \\ s_{3z} \end{bmatrix} = \begin{bmatrix} s\theta_2 \\ -s\theta_1c\theta_2 \\ c\theta_1c\theta_2 \end{bmatrix} \tag{6}$$

Then,

$$\theta_2 = \sin^{-1}(s_{3x}) \text{, and } \theta_1 = \text{Atan2}[-s_{3y} / c\theta_2, s_{3z} / c\theta_2] \tag{7}$$

From Eq. (2), we obtain

$$\boldsymbol{w}_q = R_1 R_2 R_3 R_4 R_5 \boldsymbol{w}_{q0} . \tag{8}$$

Since θ_1, θ_2, and t_3 are already known, the above equation can be reduced to

$$^3\boldsymbol{w}_q = R_4 R_5 \boldsymbol{w}_{q0} \tag{9}$$

where $^3\boldsymbol{w}_q = R_3^T R_2^T R_1^T \boldsymbol{w}_q$. So, we can obtain the following relation.

$$\begin{bmatrix} ^3w_{qx} \\ ^3w_{qy} \\ ^3w_{qz} \end{bmatrix} = \begin{bmatrix} c\theta_4 s\theta_5 \\ s\theta_4 s\theta_5 \\ c\theta_5 \end{bmatrix} \tag{10}$$

Then,

$$\theta_5 = \cos^{-1}(^3w_{qx}) \text{, and } \theta_4 = \text{Atan2}[^3w_{qy} / s\theta_5, {}^3w_{qx} / s\theta_5] \tag{11}$$

It is noted that two solution sets are possible in the working range, i.e., $\theta_5 = \theta_5^*$ or $-\theta_5^*$.

The inverse kinematics of the 3-DOF parallel manipulator is simply determined by

$$d_i = \left\| R_p \boldsymbol{b}_i + \boldsymbol{p} - \boldsymbol{a}_i \right\| \quad \text{for } i = 1,2,3 \tag{12}$$

where

$$\begin{bmatrix} R_p & \boldsymbol{p} \\ 0_{1\times 3} & 1 \end{bmatrix} = A_1(\theta_1) A_2(\theta_2) A_3(t_3) \begin{bmatrix} I_{3\times 3} & \boldsymbol{p}_0 \\ 0_{1\times 3} & 1 \end{bmatrix}, \ \boldsymbol{p}_0 = [0,0,L_0]^T,$$

$$\boldsymbol{a}_1 = r_a \begin{bmatrix} 1/2 \\ \sqrt{3}/2 \\ 0 \end{bmatrix}, \ \boldsymbol{a}_2 = r_a \begin{bmatrix} -1 \\ 0 \\ 0 \end{bmatrix}, \ \boldsymbol{a}_3 = r_a \begin{bmatrix} 1/2 \\ -\sqrt{3}/2 \\ 0 \end{bmatrix}, \text{ and}$$

$$\boldsymbol{b}_1 = r_b \begin{bmatrix} 1/2 \\ \sqrt{3}/2 \\ 0 \end{bmatrix}, \ \boldsymbol{b}_2 = r_b \begin{bmatrix} -1 \\ 0 \\ 0 \end{bmatrix}, \ \boldsymbol{b}_3 = r_b \begin{bmatrix} 1/2 \\ -\sqrt{3}/2 \\ 0 \end{bmatrix}.$$

3 Error Model

When there some kinematic errors exist in the *U-P-R-R* serial chain, the kinematic parameters for an actual model can be summarized in Table 2. For a revolute joint, four kinematic errors (two for the direction of joint axis and two for location error) can be considered, however, for a prismatic joint, only two kinematic errors for the joint direction exist. The total kinematic errors associated with directions and locations of joint axes are 18 and there are 5 joint offsets $(\delta\theta_1, \delta\theta_2, \delta t_3, \delta\theta_4, \delta\theta_5)$. Therefore, 23 kinematic errors should be estimated by the following kinematic calibration.

Once the kinematic errors in the serial chain is determined, the relation between the *U-P* chain and three *S-P-U* chains needs to be investigated. The kinematic errors in the *S-P-U* chains are summarized as follow:

Joint location errors: $\delta\boldsymbol{a}_i$ and $\delta\boldsymbol{b}_i$ for $i = 1,2,3$

Length offset errors: δd_i for $i = 1,2,3$

The kinematic errors will be determined by using Eq. (12).

Table 2 Kinematic parameters for an actual model.

Joint	$\boldsymbol{s}_i$	$\boldsymbol{s}_{0i}$
1	$(\sqrt{1-u_{1y}^2-u_{1z}^2}, u_{1y}, u_{1z})$	$(0, \delta y_1, \delta z_1)$
2	$(u_{2x}, \sqrt{1-u_{2x}^2-u_{2z}^2}, u_{2z})$	$(\delta x_2, 0, \delta z_2)$
3	$(u_{3x}, u_{3y}, \sqrt{1-u_{3x}^2-u_{3y}^2})$	$(0,0,0)$
4	$(u_{4x}, u_{4y}, \sqrt{1-u_{4x}^2-u_{4y}^2})$	$(\delta x_4, \delta y_4, 0)$
5	$(u_{5x}, \sqrt{1-u_{5x}^2-u_{5z}^2}, u_{5z})$	$(\delta x_5, 0, L_0 + L_1 + \delta z_5)$

4 Kinematic Calibration

In this work, the kinematic calibration method will be performed by using a length measurement, i.e., ball-bar [3-7]. In the following derivation, the superscripts, “*c*” and “*m*” are used to denote the calculated and measured values, respectively, and the subscript, “*j*” is employed to indicate the measurement number. As illustrated in Fig. 3, the calibration methods using length measurement is to find the set of kinematic parameters satisfying the following equation:

$$\left\| \boldsymbol{q}^c(\boldsymbol{\theta}_j^m + \delta\boldsymbol{\theta}, \boldsymbol{\beta}) - \boldsymbol{c} \right\| = l_j^m \tag{13}$$

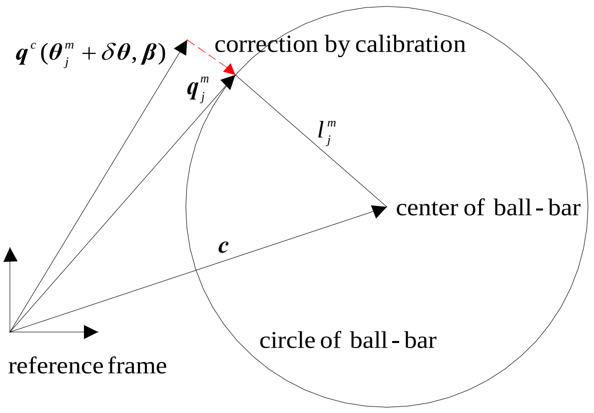

Fig. 3 Outline of the calibration methods using a ball-bar.

where $\boldsymbol{q}(\cdot)$ denotes the forward kinematics function of the *U-P-R-R* serial chain, $\boldsymbol{\theta}_j^m$ and $\delta\boldsymbol{\theta}$ denote the measured joint angle and the joint offset vectors, $\boldsymbol{\beta}$ is the kinematic error vector in Table 2 to be updated, and $\boldsymbol{c} = \bar{\boldsymbol{c}} + \delta\boldsymbol{c}$ and l_j^m denote the position vector of the fixed center of a ball-bar and the measured length of a ball-bar, respectively.

The purpose of this work is to develop and to verify the effectiveness of a kinematic calibration method suitable for the prototype of a 5-axis hybrid machine tool being developed as shown in Fig. 4. The main kinematic parameters of the machine tool are listed in Table 3.

Prior to a real calibration experiment in near future, we assume a virtual prototype with realistic kinematic errors. The error bound is determined from the information on machining and assembling tolerances and its direction is generated by the random function in Matlab. We also assume that the prototype machine will be calibrated by a ball-bar, specifically, the QC10 ball-bar of Renishaw with the accuracy, $\pm 0.5[\mu\text{m}]$. For the collection of measurement data, one center of the ball-bar is fixed at $\bar{\boldsymbol{c}} = [0, 0, 1500]^T[\text{mm}]$ expressed in the reference frame. The $n = 32$ measurement points are selected on the hemisphere surfaces with 150 mm radius. The *n* sets of encoder values from the three linear actuators and the *U-P-R-R* serial chain and the corresponding *n* ball-bar lengths are measured at the same time, which are actually calculated from the virtual prototype for numerical simulations. Using Eq. (13) and “lsqnonlin” function of Matlab, the kinematic parameters and the position error of the ball center are updated so as to minimize the error between the calculated and measured lengths of the ball-bar.

Fig. 4. Prototype of a 5-axis hybrid machine tool.

Table 3 Parameters for a prototype machine tool.

Parameters	Unit [mm]
Radius of the fixed plate (r_a)	600
Radius of the moving plate (r_b)	250
Reference height (L_0)	840
Distance between A and C (L_1)	291
Tool length (L_2)	340
Initial length of an actuator (d_{i0})	910
Linear actuator stroke (Δd_i)	800

We assume that the maximum error bounds for angle and length are $\pm 25[\text{arcsec}]$ and $\pm 25[\mu\text{m}]$, respectively. The assumed kinematic errors for a virtual prototype are written in parentheses of Table 4. The estimated kinematic parameters by the suggested calibration method are also in Table 4. It is noted that estimated values are close to the assumed ones and at least the signs are identical. It is also noted that estimated values does not necessarily following the assumed ones.

In order to show the effectiveness of the suggested calibration method, the well-known circular test on the XY plane with the radius of 150 mm is presented in Fig. 5. From the kinematic calibration and error compensation, the maximum absolute kinematic error has been reduced from $214.5[\mu\text{m}]$ to $48.2[\mu\text{m}]$.

Table 4 Assumed and estimated kinematic errors.

i	$\boldsymbol{s}_i$	Estimated (Assumed)	$\boldsymbol{s}_{0i}$	Estimated (Assumed)	$\delta\theta_i$	Estimated (Assumed)
1	u_{1y}	14.6132 (22.5065)	δy_1	-22.1156 (-16.1867)	$\delta\theta_1$	3.6879 (5.7716)
	u_{1z}	-4.7791 (-13.4431)	δz_1	-12.6657 (-4.7147)		
2	u_{2x}	13.2356 (5.3421)	δx_2	37.9109 (21.7735)	$\delta\theta_2$	9.8016 (14.5969)
	u_{2z}	-1.0796 (-0.7009)	δz_2	12.9004 (20.8452)		
3	u_{3x}	15.6955 (19.5649)			δt_3	7.7064 (15.6583)
	u_{3y}	13.4825 (13.1048)				
4	u_{4x}	-6.1924 (-2.1766)	δx_4	12.5541 (-4.4865)	$\delta\theta_4$	-1.3791 (21.0906)
	u_{4y}	-22.605 (-24.0748)	δy_4	6.9893 (19.6825)		
5	u_{5x}	1.3792 (16.0704)	δx_5	-29.9936 (-22.1054)	$\delta\theta_5$	1.5168 (11.9104)
	u_{5z}	-3.5677 (-2.7648)	δz_5	-7.3568 (-7.3566)		
	δc_x	-46.8734 (-15.5173)	δc_y	11.9864 (-15.3284)	δc_z	-7.9520 (9.1112)

[Unit: [arc sec] for angle and $[\mu\text{m}]$ for length]

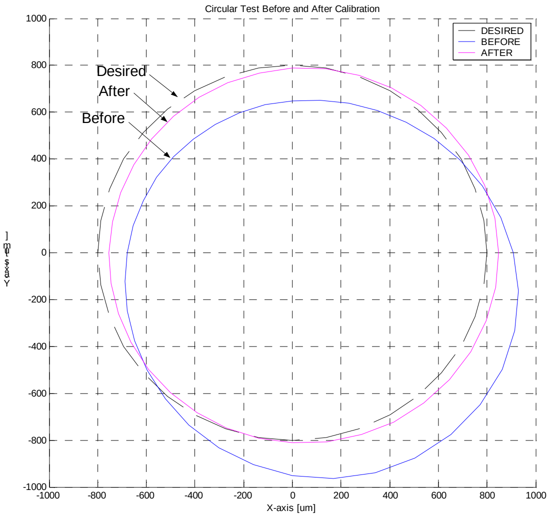

Fig. 5. Circular test before and after calibration.

Using the proposed algorithm and verified calibration procedure through simulation, calibration experiment has been performed on the prototype machine tool as shown in Fig. 6. In the experiment, The Renishaw QC10 ball-bar with ±0.5[μm] is used. The n=32 points on the hemisphere surface with radius 150 mm are collected for updating kinematic parameters. We first calibrated some major errors, for example, the offset lengths of linear actuators. Then, the well-known circular test was performed (refer to Fig. 7(a)). The circular test result after calibration experiment is shown in Fig. 7(b). From the two tests, it is verified that position accuracy of the prototype machine tool has been improved from 153 to 86 [μm].

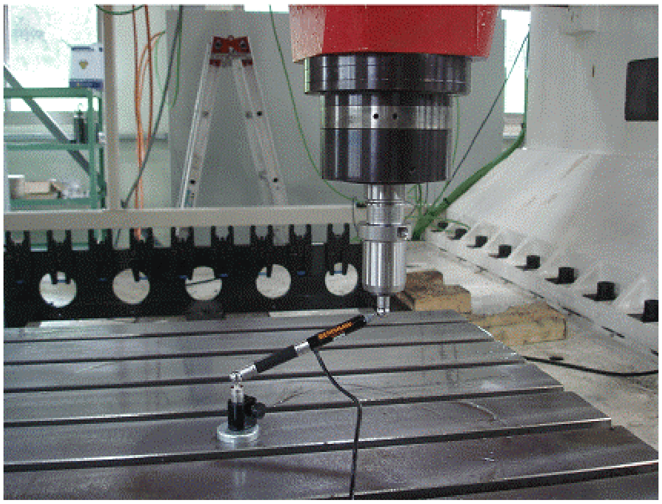

Fig. 6. Calibration experiment using a ball-bar.

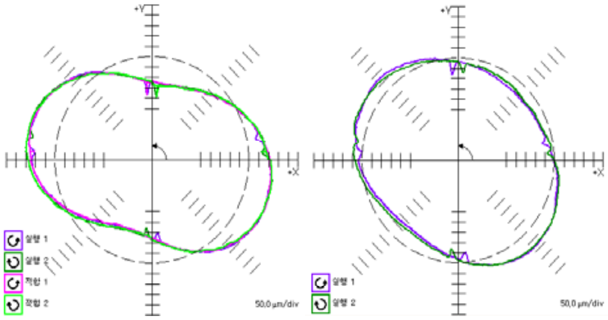

(a) before calibration (b) after calibration

Fig. 7. Circular tests with radius 150 mm.

5 Conclusion

In this paper, a new hybrid-kinematic structure for both machining and assembling is proposed. By attaching additional sensors to passive joints in the central leg, the hybrid structure can be considered as a pure serial manipulator. Using the successive screw displacements, the kinematics analysis is performed and a kinematic error model is developed for the 5-DOF serial chain. The 5-DOF serial chain is calibrated by using a length measurement, i.e., ball-bar. Once all the kinematic parameters in the serial chain are determined, the kinematic parameters associated with the parallel-kinematic manipulator will be estimated. In order to verify the effectiveness of this suggested method, the simulation results of the kinematic calibration for a virtual prototype have been presented. We further performed the calibration experiment on the prototype machine tool. From the kinematic calibration and error compensation, the maximum kinematic error has been reduced from 153 to 86 [μm].

REFERENCES

[1] L. W. Tsai, *Robot Analysis: the mechanics of serial and parallel manipulators*, Wiley, 1999.

[2] B. W. Mooring, et al, *Fundamentals of Manipulator Calibration*, Wiley, 1991.

[3] H. S. Kim, "Kinematic Calibration of a Cartesian Parallel Manipulator," *International Journal of Control, Automation, and Systems*, Vol. 3, No. 3, pp. 1-8, 2005.

[4] A. J. Patel and K. F. Ehmann, "Calibration of a Hexapod Machine Tool using a Redundant Leg," *International Journal of Machine Tools & Manufacture*, Vol. 40, pp. 489-512, 2000.

[5] Y. Takeda, G. Shen, and H. Funabashi, 2004, "A DBB-based Kinematic Calibration Method for In-Parallel Actuated Mechanisms Using Fourier Series," *Journal of Mechanical Design*, Vol. 126, No. 5, pp. 856-865

[6] B. Siciliano, 1999, "The Tricept Robot: Inverse Kinematics, Manipulability Analysis and Closed-loop Direct Kinematics Algorithm," *Robotica*, Vol. 17, pp. 437-445.

[7] L. Beyer and J. Wulfsberg, 2004, "Practical Robot Calibration with ROSY," *Robotica*, Vol. 22, pp. 505-512.